International Journal of Control, Automation and Systems VV(X) (YYYY) 1-15
http://dx.doi.org/10.1007/s12555-xxx-xxxx-x
ISSN:1598-6446 eISSN:2005-4092
http://www.springer.com/12555

A Constructive Methodology for the IDA-PBC of Underactuated 2-DoF Mechanical Systems with Explicit Solution of PDEs

Pierluigi Arpenti*, Fabio Ruggiero, and Vincenzo Lippiello

Abstract: This paper presents a passivity-based control strategy dealing with underactuated two-degree-of-freedom (2-DoF) mechanical systems. Such a methodology, which is based on the interconnection and damping assignment passivity-based control (IDA-PBC), rooted within the port-controlled Hamiltonian framework, can be applied to a very large class of underactuated 2-DoF mechanical systems. The main contribution, compared to the previous literature, is that the new methodology does not involve the resolution of any partial differential equation, since explicit solutions are given, while no singularities depending on generalised momenta are introduced by the controller. The proposed strategy is applied to two case studies: a) the stabilisation of a translational oscillator with a rotational actuator (TORA) system; b) the gait generation for an underactuated compass-like biped robot. The performances of the presented solution are evaluated through numerical simulations.

Keywords: Passivity-based control; interconnection and damping assignment; port-controlled Hamiltonian; TORA system; biped robots

1. INTRODUCTION

The interconnection and damping assignment passivity-based control (IDA-PBC) is a well-established control methodology, firstly introduced in [1], rooted within the port-controlled Hamiltonian (pH) framework of nonlinear dynamic systems. Differently from other nonlinear control methodologies, sliding mode control and feedback linearization, for example, which have been used in several applications [2], [3], [4], some of which explicitly developed for 2D nonlinear systems [5], IDA-PBC does not aim at the cancellation of nonlinear terms but, instead, it exploits the nonlinear nature of the plant. IDA-PBC brings a given nonlinear system at the desired equilibrium point by matching the original system's dynamics with those of the desired closed loop. The desired total energy in the closed loop must exhibit a minimum in such an equilibrium. The matching involves the solution of a set of partial differential equations (PDEs), called matching equations, which represent the main bottleneck of the control design. These PDEs are parameterised by three matrices that are, in general, related to the interconnection between the subsystems, the damping, and the kernel of the input matrix, respectively. These PDEs also include the plant's dynamics and the desired closed-loop total energy. Several interpretations can be given to the role played by these matrices, as explained in [6]. Throughout years, several strategies have addressed constructive procedures avoiding the solution of the PDEs [7], and they are distinguished by how the matching process is tackled. Referring to the taxonomy introduced in [6], the described methodology can be grouped into three main classes: *i)* non-parameterised IDA-PBC; *ii)* algebraic IDA-PBC; *iii)* parameterised IDA-PBC. The non-parameterised IDA-PBC represents the standard formulation proposed in [1]. In this case, the desired interconnection and the damping matrices, as well as the input matrix, are fixed. The procedure leads to a set of PDEs defining the family of the proper desired total energy functions. A solution, having a minimum in the desired equilibrium, is selected among such a family. A constructive methodology based on a dynamic extension is provided in [8], exploiting the notion of the algebraic solution of the matching equations. The authors proposed to asymptotically stabilise an equilibrium point without involving the solution of any PDE by constructing an auxiliary energy function in an extended state-space. As firstly proposed in [9], the algebraic IDA-PBC fixes the desired energy function for the closed loop. This choice transforms the matching equations into algebraic ones with the interconnection matrix, the damping matrix, and the input mapping port as unknowns. This approach, which is inherently constructive and straightforward, is based on the exact knowledge of the desired energy function that, in turn, requires proper

Manuscript received January 10, 2015; revised March 10, 2015; accepted May 10, 2015. Recommended by Associate Editor Soon-Shin Lee under the direction of Editor Milton John. This journal was supported by the Korean Federation of Science and Technology Societies Grant.

Authors are with PRISMA Lab, Department of Electrical Engineering and Information Technology, University of Naples, Via Claudio 21, 80125, Naples, Italy (e-mails: {pierluigi.arpenti, fabio.ruggiero, vincenzo.lippiello}@unina.it).
* Corresponding author.

physical considerations that are not always easy to derive. The parameterised IDA-PBC fixes the structure (*i.e.*, the family) of the desired energy function. This is convenient in those physical systems which always exhibit the same structure of the total energy. An example is given by the mechanical systems whose desired energy function is the sum of a potential energy term, depending only on the generalised positions, and the kinetic energy, which is quadratic in the generalised momenta. According to [10], relatively to the class of underactuated two-degree-of-freedom (2-DoF) mechanical systems with underactuation degree one, such a parameterisation yields to the decomposition of the original matching equations in two separate PDEs. The former is referred to as *kinetic energy matching equation* (KE-ME), and it depends on the generalised momenta; the latter is referred to as *potential energy matching equation* (PE-ME). Besides, such a parameterisation introduces some degrees of freedom which are helpful for the solution of the PDEs. Several constructive solutions were presented for this methodology. For instance, the results presented in [11] show that if the original system's inertia matrix, as well as the forces induced by the potential energy, does not depend on the unactuated coordinates, and given a particular parameterisation of the desired inertia matrix, then the KE-ME can be solved as an algebraic equation. Besides, the PE-ME admits a general solution, which is a given integral. Conversely, a solution that can be applied only to those systems having an inertia matrix depending exclusively on the unactuated coordinates, and endowing a constant sub-block matrix, is proposed in [12]. However, in this last case, the pH structure of a mechanical system in closed loop is not preserved. The recent methodology from [13] proposes a constructive solution for underactuated 2-DoF mechanical systems by relaxing some of the constraints imposed by the previous works. In particular, the plant's inertia matrix can depend on both the actuated and the unactuated variables. Such a procedure avoids the explicit solution of the matching equations by parameterising the desired inertia matrix. However, it introduces a singularity in the interconnection matrix depending on generalised momenta. In this work, a new constructive solution is designed to stabilise underactuated 2-DoF mechanical systems. Such a control law combines the main features of the parameterised IDA-PBC and the algebraic IDA-PBC. The desired closed-loop inertia matrix and the interconnection matrix are suitably parameterised to provide the solutions of the PDEs directly. In detail, an explicit solution for the PE-ME is found, while the KE-ME is transformed into an algebraic equation. Besides, singularities in the interconnection matrix are explicitly avoided. The proposed solution can be applied to a broad class of underactuated 2-DoF mechanical system, with a few assumptions on the plant's dynamics. The approach is thus tested on two mechanical systems, very different with respect to each other, namely, the translational oscillator with rotational actuator (TORA) and the underactuated compass-liked biped robot (UCBR). Numerical tests are carried out also in the presence of parametric uncertainties and noisy measurements. The same systems were already deployed by the authors in [14] and [15] to evaluate the performances of the methodology presented in [13]. Such methodology leads to a singularity, depending on generalised momenta, in the controller. The singularity has been managed numerically in [15], whereas an ad-hoc solution without singularity has been empirically found in [14]. This paper proposes the analytical procedure to design the control law without singularity structurally.

The outline of the paper is organised as follows. In Section 2 the basic concepts about IDA-PBC are illustrated. The main result is presented in Section 3, while sections 4 and 5 show two possible case studies of application, supported by the relative numerical simulations. Finally, conclusion and future work are discussed in Section 6.

2. PRELIMINARIES ON IDA-PBC FOR APPLICATIONS TO UNDERACTUATED 2-DOF MECHANICAL SYSTEMS

This section is intended to give the preliminary concepts about the IDA-PBC.

Assumptions: *The underactuated 2-DoF mechanical systems addressed in this paper have $n = 2$ degrees of freedom, $m = 1$ control inputs, no natural dissipation, constant input matrix, and continuous bounded elements of the inertia matrix.* Such assumptions are reasonable and cover a very broad class of 2-DoF mechanical systems [16]. They can be described in the pH formalism as

$$\begin{bmatrix}\dot{q}\\ \dot{p}\end{bmatrix} = \begin{bmatrix}O_2 & I_2\\ -I_2 & O_2\end{bmatrix}\nabla H(q,p) + \begin{bmatrix}0_2\\ G\end{bmatrix}u, \tag{1}$$

with $q = \begin{bmatrix}q_1 & q_2\end{bmatrix}^T \in \mathbb{R}^2$ the generalised coordinates vector, $p = \begin{bmatrix}p_1 & p_2\end{bmatrix}^T \in \mathbb{R}^2$ the generalised momenta vector, $I_k \in \mathbb{R}^{k\times k}$ and $O_k \in \mathbb{R}^{k\times k}$ the identity matrix and the zero matrix of proper dimensions, respectively, $0_k \in \mathbb{R}^k$ the zero vector of proper dimension, $G = \begin{bmatrix}1 & 0\end{bmatrix}^T \in \mathbb{R}^2$ the constant input mapping port, and $u \in \mathbb{R}$ the scalar control input. The scalar function $H(q,p) : \mathbb{R}^4 \to \mathbb{R}$ is the Hamiltonian, expressing the total mechanical energy of the original system as

$$H(q,p) = \frac{1}{2}p^T M^{-1}(q)p + V(q), \tag{2}$$

where $V(q) : \mathbb{R}^2 \to \mathbb{R}$ is the potential energy and $M(q) \in \mathbb{R}^{2\times 2}$ is the positive definite inertia matrix, whose generic element is $b_{i,j}(q)$, with $i, j = \{1,2\}$.

The IDA-PBC wants to bring the system (1) into the

desired closed-loop expression (5)

$$\begin{bmatrix}\dot{q}\\ \dot{p}\end{bmatrix}=\begin{bmatrix}O_2 & M^{-1}(q)M_d(q)\\ -M_d(q)M^{-1}(q) & J_2(q,p)-Gk_dG^T\end{bmatrix}\nabla H_d(q,p), \tag{3}$$

where $H_d(q,p):\mathbb{R}^4\to\mathbb{R}$ is the desired Hamiltonian scalar function (*i.e.*, $H_d(q,p)=\frac{1}{2}p^TM_d^{-1}(q)p+V_d(q)$ for mechanical systems), and $k_d>0\in\mathbb{R}$ is a positive damping gain. In addition, the following crucial conditions must be satisfied:

- **C.1** $M_d(q)\in\mathbb{R}^{2\times2}$ is the desired mass matrix which must be positive definite ($M_d(q)>0$) and symmetric ($M_d(q)=M_d(q)^T$);
- **C.2** $V_d(q):\mathbb{R}^2\to\mathbb{R}$ is the desired potential energy scalar function which must admit a minimum in the desired equilibrium $q^\star=\text{argmin}V_d(q)$;
- **C.3** $J_2(q,p)\in\mathbb{R}^{2\times2}$ is the assigned interconnection matrix which must be skew-symmetric ($J_2(q,p)=-J_2(q,p)^T$).

Notice that, for mechanical systems, because of **C.2**, the desired equilibrium point $(q,p)=(q^\star,0_2)$ corresponds to the minimum of the total energy $(q^\star,0_2)=\text{argmin}\,H_d(q,p)$.

Problem Statement: *Find a control-law matching the pH system* (1) *with the desired closed-loop pH system* (3)*, satisfying* ***C.1****,* ***C.2****, and* ***C.3****.*

Matching (1) with the target closed-loop (3) yields the following set of PDEs (*i.e.*, the matching equations)

$$G^\perp\left(\nabla_qH(q,p)-M_d(q)M^{-1}(q)\nabla_qH_d(q,p)+J_2(q,p)M_d^{-1}(q)p\right)=0. \tag{4}$$

Defined $G^\perp=\begin{bmatrix}0 & 1\end{bmatrix}\in\mathbb{R}^{1\times2}$ as the left annihilator of G, the matching process, as explained in the previous section, changes accordingly to the methodology adopted. Notice that, in case of fully actuated systems, the PDEs (4) are trivially satisfied since $G^\perp$ is a null matrix. Therefore, the potential and kinetic energies can be shaped as desired. In general, for fully actuated system, only the potential energy is shaped to avoid nonlinear cancellations, reducing the robustness of the closed loop. The non-parameterised IDA-PBC fixes the structure of $J_2(q,p)$ in (4), defining the family of admissible $H_d(q,p)$ satisfying the matching equations. The algebraic IDA-PBC fixes the desired total energy $H_d(q,p)$ exactly. For mechanical systems, this means that $M_d(q)$ and $V_d(q)$ are previously defined. In this way, the matching equations (4) become algebraic with $J_2(q,p)$ as unknown. The parameterised IDA-PBC fixes the structure of $H_d(q,p)$. For mechanical systems, this means that a parameterisation of $M_d(q)$ and $V_d(q)$ is defined. This splits the matching equations (4) into two subsets of PDEs, namely the KE-ME

$$G^\perp(\nabla_q(p^TM^{-1}(q)p)-M_d(q)M^{-1}(q)\nabla_q(p^TM_d^{-1}(q)p)+2J_2(q,p)M_d^{-1}(q)p)=0,$$

and the PE-ME

$$G^\perp(\nabla_qV(q)-M_d(q)M^{-1}(q)\nabla_qV_d(q))=0. \tag{6}$$

Both the KE-ME and the PE-ME are solved with respect to the chosen parameterisation for $M_d(q)$ and $V_d(q)$, which in turn gives some constraints on $J_2(q,p)$ as clear from (5).

Regardless of the chosen approach, at the end of the matching process, the terms $V_d(q)$, $M_d(q)$, and $J_2(q,p)$ are known. Hence, the energy-shaping control law can be computed as

$$u_{es}=(G^TG)^{-1}G^T(\nabla_qH(q,p)-M_d(q)M^{-1}(q)\nabla_qH_d(q,p)+J_2(q,p)M_d^{-1}(q)p), \tag{7}$$

which defines a strict minimiser of the potential energy in the desired equilibrium $(q,p)=(q^\star,0_2)$. Moreover, a damping injection term

$$u_{di}=-k_dG^T\nabla_pH_d(q,p) \tag{8}$$

guarantees the asymptotic stability of the desired equilibrium if the passive output

$$y_d(q,p)=G^T\nabla_pH_d(q,p)=G^TM_d^{-1}(q)p \tag{9}$$

is detectable (see Remark 3.2.21 in [17]). The final control law is thus

$$u=u_{es}+u_{di}. \tag{10}$$

For more details see [10].

The key idea of the proposed methodology, described in the the next section, is to combine the advantages of the parameterised IDA-PBC and the algebraic IDA-PBC. After giving a suitable parameterisation for $M_d(q)$ complying with **C.1**, it is possible to retrieve a family for the desired potential energy $V_d(q)$ in which impose the condition **C.2**. For the considered 2-DoF mechanical systems, in order to comply with **C.3**, the interconnection matrix can be uniquely defined as

$$J_2=\begin{bmatrix}0 & j_2(q,p)\\ -j_2(q,p) & 0\end{bmatrix}, \tag{11}$$

where $j_2(q,p):\mathbb{R}^4\to\mathbb{R}$ is a scalar function. Having at disposition both $M_d(q)$ and $V_d(q)$, as for the algebraic IDA-PBC, the KE-ME becomes an algebraic equation in $j_2(q,p)$

$$G^\perp\nabla_q\left(p^TM^{-1}(q)p\right)-G^\perp M_d(q)M^{-1}(q)\nabla_q\left(p^TM_d^{-1}(q)p\right)-2j_2(q,p)G^TM_d^{-1}p=0, \tag{12}$$

whose solution is given by

$$j_2(q,p) = \frac{G^\perp(\nabla_q(p^T M^{-1}(q)p) - M_d(q)M(q)^{-1}\nabla_q(p^T M_d^{-1}(q)p))}{2G^T M_d^{-1}(q)p}. \tag{13}$$

Such a solution exhibits a singularity in the generalised momenta p

$$\begin{aligned} &G^T M_d^{-1}(q)p = 0 \Rightarrow \\ &\begin{bmatrix} 1 & 0 \end{bmatrix} \begin{bmatrix} m_{d22}(q) & -m_{d12}(q) \\ -m_{d12}(q) & m_{d11}(q) \end{bmatrix} \begin{bmatrix} p_1 \\ p_2 \end{bmatrix} = 0 \\ &\iff (m_{d22}(q)p_1 - m_{d12}(q)p_2) = 0. \end{aligned} \tag{14}$$

Hence, the singularity appears when either $m_{d22}(q)p_1 = m_{d12}(q)p_2$ or the system is at the equilibrium, $p^\star = 0_2$. The former condition is not predictable a priori. The latter is a consequence of the detectability-like condition required to guarantee the asymptotic stability of the closed-loop equilibrium when (8) is introduced in the control action. Such a condition requires that the passive output $y_d = G^T M_d^{-1}(q)p$, which is exactly the denominator of (13), nullifies at the equilibrium. This singularity due to the generalised momenta p is a problem for mechanical systems and it is present in many works [10, 13, 15, 18]. In these papers, the problem was worked around either numerically or with ad-hoc solution for the peculiar addressed case-study. In the next section, it will be shown how the presented methodology can remove such a singularity in p structurally. Notice that further fractional functions may be introduced within (13) from the choice of $M_d(q)$: singularities in the generalised coordinates q must be managed during the design of the target inertia matrix.

Remark. *This work deals with undamped systems. This is the standard in IDA-PBC literature, due to the additive complexity in solving matching equations which arises when accounting for natural dissipation. An extension to IDA-PBC is presented in [19], with conditions for the existence of a control redesign capable of handling damping terms in the original system. Such extension is beyond the scope of the work and will not be further considered.*

3. MAIN RESULT

Notation remark. *In this section, with a little abuse of notation, it will also be highlighted the dependency on some parameters to be tuned. Besides, in the following, given a generic function $f(q)$, the notation $f(\begin{bmatrix} q_a & q_b \end{bmatrix})$ means that the variable q_1 is substituted by q_a and the variable q_2 is substituted by q_b, respectively.* As explained before, the key idea is to combine the advantages of both the parameterised IDA-PBC and the algebraic IDA-PBC, solving each singularity issue. Hence, the resulting approach provides an explicit solution of the PE-ME and requires to solve the KE-ME as an algebraic equation, just like the algebraic IDA-PBC does, without assigning the exact values of $M_d(q)$ and $V_d(q)$, in the spirit of the parameterised IDA-PBC, and without introducing any singularity in $j_2(q,p)$. As expressed in [13], the starting point is the parameterisation of the desired inertia matrix in (3) as

$$M_d(q,c_1) = \Delta(q) \begin{bmatrix} a_{11}(q,c_1) & a_{12}(q,c_1) \\ a_{12}(q,c_1) & a_{22}(q,c_1) \end{bmatrix} \tag{15}$$

where $\Delta(q) = b_{11}(q)b_{22}(q) - b_{12}(q)^2$ is the determinant of $M(q)$, $c_1 \in \mathbb{R}^{n_{c_1}}$ is a set of gains useful to design the controller, with $n_{c_1} > 0$, and $a_{ij}(q,c_1) \in \mathbb{R}$ are scalar functions to be defined and related to $M_d(q,c_1)$. Under this parameterisation, the PE-ME (6) becomes

$$G^\perp(\nabla_q V(q) - \Gamma(q,c_1)\nabla_q V_d(q,c_2)) = 0, \tag{16}$$

with $c_2 \in \mathbb{R}^{n_{c_2}}$ a set of gains useful to design the controller, with $n_{c_2} > 0$, and

$$\Gamma(q,c_1) = M_d(q,c_1)\, M(q)^{-1} = \begin{bmatrix} \Gamma_{11}(q,c_1) & \Gamma_{12}(q,c_1) \\ \Gamma_{21}(q,c_1) & \Gamma_{22}(q,c_1) \end{bmatrix} \tag{17}$$

where

$$\begin{aligned} \Gamma_{11}(q,c_1) &= a_{11}(q,c_1)b_{22}(q) - a_{12}(q,c_1)b_{12}(q), \\ \Gamma_{12}(q,c_1) &= a_{12}(q,c_1)b_{11}(q) - a_{11}(q,c_1)b_{12}(q), \\ \Gamma_{21}(q,c_1) &= a_{12}(q,c_1)b_{22}(q) - a_{22}(q,c_1)b_{12}(q), \\ \Gamma_{22}(q,c_1) &= a_{22}(q,c_1)b_{11}(q) - a_{12}(q,c_1)b_{12}(q). \end{aligned}$$

The key of the approach is to introduce a scalar function $\gamma(q,c_1) \in R$ that parameterises the second row of $\Gamma(q,c_1)$ as

$$a_{22}(q,c_1)b_{12}(q) - a_{12}(q,c_1)b_{22}(q) = k_1\gamma(q,c_1), \tag{18a}$$

$$a_{12}(q,c_1)b_{12}(q) - a_{22}(q,c_1)b_{11}(q) = k_2\gamma(q,c_1), \tag{18b}$$

with $k_1, k_2 \in \mathbb{R}$ and $k_1 \neq 0$. The specific case with $k_1 = 0$ and $k_2 \neq 0$ is presented in the next subsection. Such a choice simplifies (16) as

$$\nabla_{q_2} V(q) + \gamma(q,c_1)(k_1\nabla_{q_1} V_d(q,c_2) + k_2\nabla_{q_2} V_d(q,c_2)) = 0, \tag{19}$$

whose explicit solution is

$$\begin{aligned} V_d(q,c_2) = &- \int_1^{q_1} \frac{\nabla_{q_2} V\left(\begin{bmatrix} \sigma & \dfrac{k_1q_2 - k_2q_1 + k_2\sigma}{k_1} \end{bmatrix}\right)}{k_1\gamma\left(\begin{bmatrix} \sigma & \dfrac{k_1q_2 - k_2q_1 + k_2\sigma}{k_1} \end{bmatrix}\right)} \mathrm{d}\sigma \\ &+ f_1\left(\frac{k_1q_2 - k_2q_1}{k_1}, c_2\right), \end{aligned} \tag{20}$$

with $f_1(\cdot,\cdot) \in \mathbb{R}$ any scalar function of its arguments.

Indeed, the PDE (19) admits an explicit solution provided that a right $\gamma(q,c_1)$ is found to: *(i)* guarantee a closed-form solution for the integral in (20); *(ii)* shape $V_d(q,c_2)$ such as to comply with **C.2**; and *(iii)* avoid the singularity in the interconnection matrix. The fulfilment of the first requirement is explained in Appendix A.1. Concerning the second requirement, the degrees of freedom given by $f_1(\cdot,\cdot)$ and $\gamma(q,c_1)$ may help in satisfying **C.2** as well as to avoid singularities in the generalised coordinates q. Otherwise, other choices for $\gamma(q,c_1)$ must be done. The fulfilment of the last requirement is addressed in the following. For the moment, consider that the $V_d(q,c_2)$ is found. Then, the desired inertia matrix can be computed through (15) and (18). In particular, it is possible to retrieve the scalar functions $a_{12}(q,c_1)$ and $a_{22}(q,c_1)$ as

$$a_{12}(q,c_1) = -\frac{k_1\gamma(q,c_1)b_{11}(q) + k_2\gamma(q,c_1)b_{12}(q)}{\Delta(q)}, \tag{21a}$$

$$a_{22}(q,c_1) = -\frac{k_1\gamma(q,c_1)b_{12}(q) + k_2\gamma(q,c_1)b_{22}(q)}{\Delta(q)}, \tag{21b}$$

while $a_{11}(q,c_1)$ is left free such as to satisfy **C.1**. If it is not possible to find a desired inertia matrix which matches the criteria expressed by **C.1**, it is then necessary to design again the set of gains c_1, as well as, the scalar function $f_1(\cdot,\cdot)$, and eventually $\gamma(q,c_1)$, until both **C.1** and **C.2** are simultaneously met. Once that $M_d(q,c_1)$ and $V_d(q,c_2)$ are found, the KE-ME (12) is an algebraic equation with $j_2(q,p)$ as unknown and whose solution is (13). However, as said, the solution (13) suffers of a singularity problem. To avoid this, a suitable $\gamma(q,c_1)$ must be found to fix this problem. Therefore, not any $\gamma(q,c_1)$ can be thus considered to deal with **C.1** and **C.2** through $M_d(q)$ and $V_d(q,c_1)$ in (21) and (20), respectively. The key for the solution is to recognise $j_2(q,p)$ as a fractional function

$$\begin{aligned} j_2(q,p) &= \frac{n(q,p)}{d(q,p)} \\ &= \frac{G^{\perp}(\nabla_q(p^T M^{-1}(q)p) - M_d(q)M(q)^{-1}\nabla_q(p^T M_d^{-1}(q)p))}{2G^T M_d^{-1}(q)p}. \end{aligned} \tag{22}$$

Let $\zeta(q,p) \in \mathbb{R}$ and $\eta(q,p) \in \mathbb{R}$ the quotient and the reminder of $j_2(q,p)$, respectively. The expression (22) becomes

$$\frac{n(q,p)}{d(q,p)} = \zeta(q,p) + \frac{\eta(q,p)}{d(q,p)}. \tag{23}$$

Nullifying the remainder $\eta(q,p)$ brings the solution $\eta(q,p) = 0$ implying $j_2(q,p) = \zeta(q,p)$, which is structurally not affected by any singularity in p. Taking into account (21) and (22), the equation $\eta(q,p) = 0$ to nullify the remainder can be written as

$$\begin{aligned} &\gamma(q,c_1)(k_1\gamma(q,c_1)(-k_1\nabla_{q_2}b_{11}(q) \\ &- k_2\nabla_{q_2}b_{12}(q) + k_1\nabla_{q_1}b_{12}(q) + k_2\nabla_{q_1}b_{22}(q)) \\ &+ (k_1b_{12}(q) + k_2b_{22}(q))(k_2\nabla_{q_2}\gamma(q,c_1) \\ &+ k_1\nabla_{q_1}\gamma(q,c_1))) = 0, \end{aligned} \tag{24}$$

which is a PDE in the scalar function $\gamma(q,c_1)$. The PDE (24) has two explicit solutions. The first one is trivial, $\gamma(q,c_1) = 0$, and it is not allowed because it would imply both (21a) and (21b) to be zero, preventing the fulfilling of **C.1**. The second solution is

$$\gamma(q,c_1) = f_2(q,c_1)f_3\left(\frac{k_1q_2 - k_2q_1}{k_1}, c_1\right), \tag{25}$$

where $f_3(\cdot,\cdot) \in \mathbb{R}$ is any scalar, continuous, and nonzero function of its arguments, while $f_2(q,c_1)$ is

$$\begin{aligned} f_2(q,c_1) = \exp\Bigg(\int_1^{q_1} &\frac{k_1(\nabla_{q_2}b_{11}(\cdot) - \nabla_{q_1}b_{12}(\cdot))}{k_1b_{12}(\cdot) + k_2b_{22}(\cdot)} \\ &+ \frac{k_2(\nabla_{q_2}b_{12}(\cdot) - \nabla_{q_1}b_{22}(\cdot))}{k_1b_{12}(\cdot) + k_2b_{22}(\cdot)}\mathrm{d}\sigma\Bigg), \end{aligned} \tag{26}$$

where $b_{ij}(\cdot) = b_{ij}(\begin{bmatrix}\sigma & f_4(q,\sigma)\end{bmatrix})$ to compact notation, with $i,j = \{1,2\}$, $\exp(k) = e^k$, and $f_4(q,\sigma) = (k_1q_2 - k_2q_1 + k_2\sigma)/k_1$. The expression (26) holds if the integral exists: the discussion and the proof is within Appendix A.2. The solution (25) gives the structure on how construct $\gamma(q,c_1)$ to avoid the singularity in $j_2(q,p)$. Hence, the function $\gamma(q,c_1)$ is given by two parts: *(i)* $f_2(q,c_1)$ that is fixed by (26) depending on k_1, k_2, and $M(q)$; *(ii)* $f_3(\cdot,\cdot)$ that is free to be chosen to comply with **C.1** and **C.2** through $V_d(q,c_2)$ and $M_d(q,c_1)$ in (20) and (21), respectively. The gains are also useful to avoid singularities in the generalised coordinates q within the introduced functions. Any other choice of $\gamma(q,c_1)$ may bring to a valid controller, but resulting in $j_2(q,p)$ with a singularity in the generalised momenta that has to be managed in other ways [13]. Finally, once got $j_2(q,p)$ as in (22), being sure that no singularity in p will appear, the control law can be computed as in (10). The flow-chart represented in Figure 1 resumes the derived constructive solution, which existence is guaranteed by the existence of the integrals within equations (20) and (26) (see Appendix).

The novelties introduced within this methodology do not jeopardise the property of asymptotic stability of the sought equilibrium guaranteed by the introduction of the u_{di} control term. To check the detectability of the passive output (9), it is sufficient to show that $q \to q^\star$ when $y_d = 0$. Recalling the expression of y_d in (9), since $M_d(q)$ is always positive definite because of **C.1**, then $y_d = 0 \iff p = 0_2$. When $p = 0_2$, the closed-loop (3) becomes

$$\begin{bmatrix} 0_2 \\ -M_d(q,c_1)M(q)^{-1}\nabla_q V_d(q,c_2) \end{bmatrix} = 0_4. \tag{27}$$

Given the expression of the target closed-loop Hamiltonian function $H_d(q,p) = \frac{1}{2}p^T M_d(q,c_1)p + V_d(q,c_2)$, the equations in the last two rows of (27) are satisfied if one of the following relationships holds:

1. $\det(-M_d(q,c_1)M(q)^{-1}) = 0$;
2. $\nabla_q V_d(q,c_2) = 0_2$.

The former condition is not met because it requires that $\det(M_d(q,c_1)) = 0$ which is false because **C.1** holds. The latter is satisfied at the equilibrium $q^\star$ because of the validity of **C.2**. Hence, the detectability condition of the passive output is locally guaranteed: the desired equilibrium is locally asymptotically stable with a basin of attraction that can be estimated using the LaSalle's invariance principle, as shown in [1, 17].

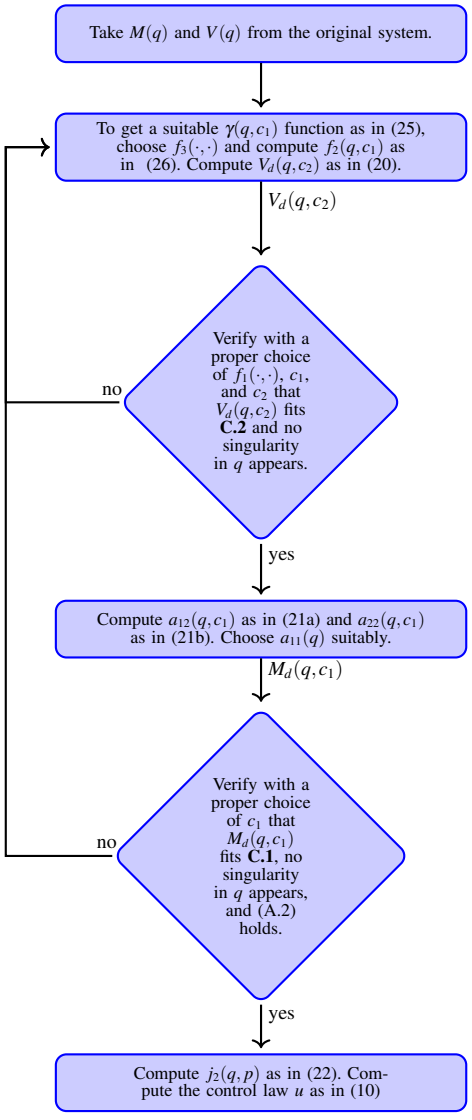

Fig. 1. Flow chart of the proposed constructive solution.

Remark *The proposed methodology can be applied to underactuated mechanical system in the form* (1)*. Indeed, the parameterisation of the desired inertia matrix does not pose limits on the applicability range of such a methodology. Besides, unlike the method proposed in [13], it does not introduce any singularity depending on generalised momenta in the control law.*

3.1. Constructive Methodology with $k_1 = 0$ and $k_2 \neq 0$

A particular solution can be achieved through the choice $k_1 = 0$ and $k_2 \neq 0$. In detail, the expressions (18) become

$$a_{22}(q,c_1)b_{12}(q) - a_{12}(q,c_1)b_{22}(q) = 0, \tag{28a}$$
$$a_{12}(q,c_1)b_{12}(q) - a_{22}(q,c_1)b_{11}(q) = k_2\gamma(q,c_1), \tag{28b}$$

Such a choice further simplifies (19) as

$$\nabla_{q_2} V(q) + \gamma(q,c_1)k_2\nabla_{q_2}V_d(q,c_2) = 0, \tag{29}$$

whose explicit solution is

$$V_d(q,c_2) = -\int_1^{q_2} \frac{\nabla_{q_2} V\left(\begin{bmatrix}\sigma & q_1\end{bmatrix}\right)}{k_2\gamma\left(\begin{bmatrix}\sigma & q_1\end{bmatrix}\right)}\mathrm{d}\sigma + f_1(q_1,c_2), \tag{30}$$

with $f_1(q_1,c_2) \in \mathbb{R}$ is now function of q_1 only and some gains. Once that the $V_d(q,c_2)$ is found and **C.2** is established, the desired inertia matrix can be computed as done for $k_1 \neq 0$. The scalar functions $a_{12}(q,c_1)$ and $a_{22}(q,c_1)$ are now equal to

$$a_{12}(q,c_1) = -\frac{k_2\gamma(q,c_1)b_{12}(q)}{\Delta(q)}, \tag{31a}$$
$$a_{22}(q,c_1) = -\frac{k_2\gamma(q,c_1)b_{22}(q)}{\Delta(q)}, \tag{31b}$$

while $a_{11}(q,c_1)$ is left free to satisfy **C.1**. The remaining part of the procedure is the same. Therefore, once that $M_d(q,c_1)$ and $V_d(q,c_2)$ are found, the function $j_2(q,p)$ should be computed. However, the function $\gamma(q,c_1)$ should be chosen properly to avoid singularity in the generalised momenta in the denominator of $j_2(q,p)$. Following the same idea, the equation to nullify the remainder (24) simplifies into $k_2^2\gamma(q,c_1)b_{22}(q)\nabla_{q_2}\gamma(q,c_1) = 0$ which is a PDE in the scalar function $\gamma(q,c_1)$. The previous PDE has again two explicit solutions. The first is trivial, $\gamma(q,c_1) = 0$, and it is not allowed because it would imply (31a) and (31b) to be zero, preventing the fulfilling of **C.1**. The latter solution is $\gamma(q,c_1) = f_3(q_1,c_1)$, where now $f_3(q_1,c_1) \in \mathbb{R}$ is any scalar, continuous, and nonzero function of q_1 only and some gains. Therefore, in the particular case $k_1 = 0$ and $k_2 \neq 0$, the degrees of freedom given by $f_1(\cdot,\cdot)$ and $\gamma(\cdot,\cdot)$ depend on q_1 only and some gains. These should be employed to fulfil **C.1** and **C.2**, as well as to avoid singularities in q. Notice that, given the arguments in the Appendix, the existence of the integral within (30) is trivial. The flow-chart represented in Figure 1 holds also in the case of $k_1 = 0$ and $k_2 \neq 0$ with the

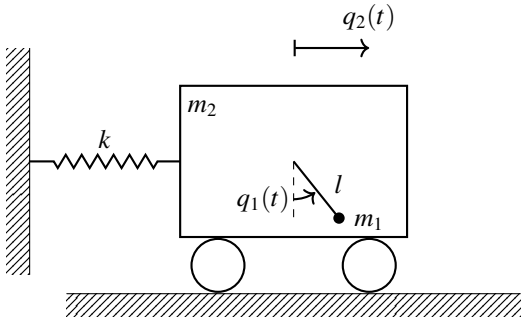

Fig. 2. Scheme of a translational oscillator with a rotational actuator system.

described changes. The possibility of choosing $k_1 = 0$ and $k_2 \neq 0$ or not depends on the particular case study. It indeed simplifies the solution but bestows fewer degrees of freedom to the control design. In the following, both approaches will be employed for two different case studies.

4. CASE STUDY A: THE TORA SYSTEM

4.1. Dynamic Model of the TORA

The TORA is an underactuated 2-DoF mechanical system firstly studied in [20] and commonly employed in the literature as a benchmark for several nonlinear control systems designs addressing underactuation. The TORA consists of a translational oscillating cart with mass $m_2 > 0$ that is controlled via a rotational eccentric mass, here schematised by a pendulum with mass $m_1 > 0$, radius $r > 0$, inertia $I = m_1 r^2$, and a rigid link to the cart of length $l > 0$. The (actuated) variable $q_1(t)$ denotes the angle of the mass m_1 with respect to the vertical, while the displacement of the cart with mass m_2 is denoted by the (unactuated) variable $q_2(t)$. The relative generalised momenta are identified by p_1 and p_2, respectively. The cart is forced to oscillate in the horizontal plane by a spring with elastic coefficient $k > 0$. The actuated eccentric mass damps the horizontal oscillations of the platform. The TORA is illustrated in Figure 2. A standard IDA-PBC approach, where the complexity of the kinetic energy matching equations is reduced by choosing a constant closed-loop mass matrix, is proposed in [21]. In [15], instead, the constructive procedure from [13] is applied to stabilise the TORA system at the equilibrium point, resulting in a controller which numerically manages the singularity appearing at the denominator of (22). A dynamic extension is proposed in [22] to achieve the asymptotic stabilisation of the system with only position measurements. The resulting controller is independent by the velocity measurements because they are not present in the potential energy due to a procedure that shapes the potential energy only, equates $M(q)$ and $M_d(q)$, and cancels the assigned interconnection matrix to get rid of the kinetic energy PDEs. Besides, different feedback-stabilizing controllers were tested on the TORA system [23]. Several controllers based on cascade (linear cascade control, integrator backstepping) and passivity (feedback passivisation, passivisation without cancellation) paradigms can be used to asymptotically stabilise the system. The former class requires full state feedback linearization and nonlinearities cancellation. In contrast, the latter class leads to controllers with a reduced set of measurements and no cancellations, for input-output passive systems with relative degree one and weakly minimum-phase. A partial feedback linearization along with a Lagrangian-based change of coordinates is addressed in [24] to reshape the system as a nonlinear cascade system in a strict-feedback form. The same change of coordinates plus a dynamic surface control is proposed in [25] to ensure exponential stability. An experimental output regulation for the TORA system is performed in [26], while a piece-wise multilinear model is considered in [27]. Finally, fuzzy control is proposed in [28].

The pH model of the TORA system is given by (1) with the elements of $M(q)$ given below

$$b_{11} = m_1 l^2 + I, b_{12}(q) = m_1 l \cos(q_1), b_{22} = m_1 + m_2. \quad (32)$$

The Hamiltonian function $H(q)$ for the TORA is equivalent to (2), with

$$V(q) = \frac{1}{2} k q_2^2 + m_1 l g (1 - \cos(q_1)). \quad (33)$$

4.2. Control Design for the TORA

Without loss of generality, the procedure presented in this paper is applied to stabilise the TORA at the desired equilibrium point $(q^\star, p^\star) = (\pi, 0, 0, 0)$. The following procedure assumes $k_1 \neq 0$. To get a proper function $\gamma(q)$, a constant $f_3((k_1 q_2 - k_2 q_1)/k_1) = k_3$ is picked up, with $k_3 \neq 0$ a suitable gain. Taking into account (32), the expression (26) becomes $f_2(q) = 1/(k_2(m_1 + m_2) + k_1 m_1 l \cos q_1)$, with $k_2 > k_1 m_1 l/(m_1 + m_2)$ to avoid any singularity in $f_2(q)$. Then, the suitable scalar function $\gamma(q, c_1)$ in (25) becomes $\gamma(q) = k_3/(k_2 b_{22} + k_1 l m_1 \cos q_1)$. The $f_1((k_1 q_2 - k_2 q_1)/k_1)$ function in (20) is chosen as follows

$$f_1\left(\frac{k_1 q_2 - k_2 q_1}{k_1}\right) = k_4 \left(\frac{k_1 q_2 - k_2 q_1}{k_1}\right)^2, \quad (34)$$

with $k_4 \in \mathbb{R}$ a suitable gain. With the above choice and expressions, the desired potential energy in (20) is

$$V_d(q) = \frac{b_{22} k k_2^2 q_1^2 - 2 b_{22} k k_1 k_2 q_1 q_2 - 2 k k_1 k_2 l m_1 \cos q_1}{2 k_1^2 k_3} + \frac{-2 k k_1^2 l m_1 q_2 \sin q_1 + 2 k_1^2 k_3 k_4 \left(\frac{k_1 q_2 - k_2 q_1}{k_1}\right)^2}{2 k_1^2 k_3}. \quad (35)$$

The evaluation of the gradient $\nabla_q V_d(q)$ in $q^\star = (\pi, 0)$ yields

$$\nabla_q V_d(q)\Big|_{q^\star} = \begin{bmatrix} \dfrac{k_2^2(b_{22}k + 2k_3k_4)\pi}{k_1^2 k_3} \\ -\dfrac{k_2(b_{22}k + 2k_3k_4)\pi}{k_1 k_3} \end{bmatrix}, \tag{36}$$

which becomes $\nabla_q V_d(q)\Big|_{q^\star} = 0_2$ if the condition $k_4 = -b_{22}k/(2k_3)$ holds. The Hessian of $V_d(q)$, evaluated in $q^\star = (\pi, 0)$, is

$$\nabla_q^2 V_d(q)\Big|_{q^\star} = \begin{bmatrix} \dfrac{2b_{22}kk_2^2 + 4k_2^2k_3k_4 - 2kk_1k_2m_1l}{2k_1^2k_3} & \\ \dfrac{-2b_{22}kk_1k_2 - 4k_1k_2k_3k_4 + 2kk_1^2m_1l}{2k_1^2k_3} & \\ & \dfrac{-2b_{22}kk_1k_2 - 4k_1k_2k_3k_4 + 2kk_1^2m_1l}{2k_1^2k_3} \\ & 2k_4 \end{bmatrix}. \tag{37}$$

This last is positive definite if the conditions

$$k_1 > 0, k_2 > \frac{k_1 m_1 l}{b_{22}}, k_3 < 0, k_4 = -\frac{b_{22}k}{2k_3} \tag{38}$$

are met. Since these conditions are not in contrast with the ones found previously for the same gains, the procedure can continue. The condition **C.2** is thus checked.

The scalar functions $a_{12}(q)$ and $a_{22}(q)$ are evaluated using (21), while $a_{11}(q)$ is free and it is here computed as proposed in [13] $a_{11}(q) = k_5 a_{12}^2(q)/a_{22}(q)$ with $k_5 \neq 0$ a suitable gain. With the above choices, the desired inertia matrix is

$$M_d(q) = \begin{bmatrix} -\dfrac{k_3k_5(b_{11}k_1 + k_2m_1l\cos q_1)^2}{(b_{22}k_2 + k_1m_1l\cos q_1)^2} & \\ -\dfrac{k_3(b_{11}k_1 + k_2m_1l\cos q_1)}{b_{22}k_2 + k_1m_1l\cos q_1} & \\ & -\dfrac{k_3(b_{11}k_1 + k_2m_1l\cos q_1)}{b_{22}k_2 + k_1m_1l\cos q_1} \\ & -k_3 \end{bmatrix}, \tag{39}$$

whose determinant is equal to $\Delta_d(q) = (k_3^2(-1 + k_5)(b_{11}k_1 + k_2m_1l\cos q_1)^2)/(b_{22}k_2 + k_1m_1l\cos q_1)^2$. To comply with **C.1**, it should be proven that the desired inertia matrix is positive definite. Thanks to the Sylvester's criterion, this is true if both $a_{11}(q) > 0$ and $\Delta_d(q) > 0$. Given (38), the former is true if

$$k_2 \neq \frac{k_1(l^2 + r^2)}{l}, k_5 > 0. \tag{40}$$

On the other hand, the latter condition is true if $k_5 > 1$. Therefore, $k_2 \neq \dfrac{k_1(l^2 + r^2)}{l}$ and $k_5 > 1$ are the conditions to fulfil **C.1**. The interconnection term $j_2(q, p)$ in (22) becomes

$$j_2(q, p) = \frac{k_1(-b_{11}k_1^2 + b_{22}k_2^2)k_3p_1m_1l\sin q_1}{(b_{22}k_2 + k_1m_1l\cos q_1)^2(b_{11}k_1 + k_2m_1l\cos q_1)}, \tag{41}$$

which does not show any dependence on the generalised momenta at the denominator and, therefore, on the passive output, as expected. However, to avoid any singularity in the q variables, the conditions $k_2 > k_1m_1l/b_{22}$ and $k_2 \neq k_1(l^2 + r^2)/l$ must hold. Both the conditions can be dropped because already contained within (38) and (40), respectively. Therefore, the set of gains avoiding any singularities and satisfying **C.1**, **C.2**, and **C.3** are

$$\begin{aligned} &k_1 > 0,\ k_2 > \frac{k_1m_1l}{m_1 + m_2} \wedge k_2 \neq \frac{k_1(l^2 + r^2)}{l},\ k_3 < 0, \\ &k_4 = -\frac{b_{22}k}{2k_3},\ k_5 > 1. \end{aligned} \tag{42}$$

Notice that the constant terms b_{11} and b_{22} were often not explicitly expressed due to space constraints. In addition, the condition $k_2 > k_1m_1l/(m_1 + m_2)$ agrees with (A.2), ensuring the existence of the integral in (26) and in (20).

Finally, the sum between the energy shaping (7) and the damping injection (8) is the total control action. The Mathematica code for the derived controller is released as a multimedia attachment. The code may be useful as a template for other case studies.

4.3. Simulations for the Controlled TORA

The current section aims to demonstrate the effectiveness of the designed controller for the TORA. To recap, the sought control goal is to stabilise the system, described by (33) and (32) at the desired equilibrium point $(q^\star, p^\star) = (\pi, 0, 0, 0)$. The nominal dynamic parameters chosen for the TORA model are $m_1 = 1$ kg, $m_2 = 10$ kg, $l = 1$ m, $r = 0.1$ m, $k = 5$ and $g = 9.81$ m/s^2. The performance of the proposed control law is evaluated in presence of parametric uncertainties, noisy measurements, and a time delay introduced by the discretization of the controller. The test is carried out on a standard personal computer in the MATLAB/Simulink environment using the *ODE*45 routine. The robustness in the presence of parametric uncertainties is tested by considering, in the control law, an increment of the 20 % in the value of the parameters m_1, m_2, l, r and k contained inside the model. Moreover, in order to evaluate the performance in presence of noisy measurements, a white noise is added to the signals $q_1(t)$, $q_2(t)$, $p_1(t)$ and $p_2(t)$, with a variance of 0.05, 0.01, 0.05, and 0.01, respectively. The discretization of the controller is also taken into account by sampling the control law each

0.01 s. The controller has been designed with gains $k_1 = 1$, $k_2 = 0.14$, $k_3 = -1$, $k_4 = 39.6$, $k_5 = 2$, $k_d = 20$. They comply with the conditions in (42). The simulation starts with initial conditions $q_1(0) = \pi/2$ rad, $q_2(0) = 0.1$ m, $p_1(0) = 0 \ \frac{kg\ rad}{s}$, $p_2(0) = 0 \ \frac{kg\ m}{s}$ and lasts for 100 s. Figure 3 depicts the time evolution of the closed-loop systems potential energy which, as expected, reaches its local minimum located in $q^\star$. As shown in Fig.4, the state trajectories of the system asymptotically converge to the desired values in roughly 40 s, with performance comparable with the methodologies belonging to the state of art in the control of the TORA, exhibiting small amplitude oscillations due to the presence of noisy measures.

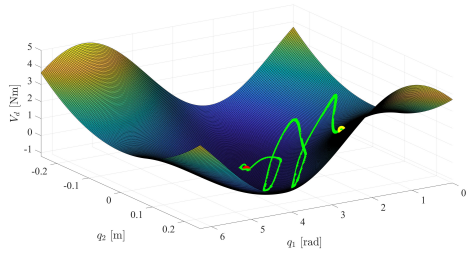

(a) Front view of $V_d(q)$ surface.

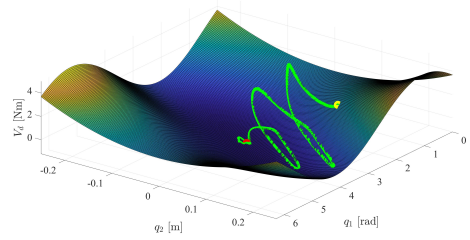

(b) Top view of $V_d(q)$ surface.

Fig. 3. Case Study A. Evolution of the closed-loop system potential energy during a test carried out with perturbed conditions. Potential energy (the green curve) evolves from its initial value (the yellow dot) until it reaches its minimum (the red dot).

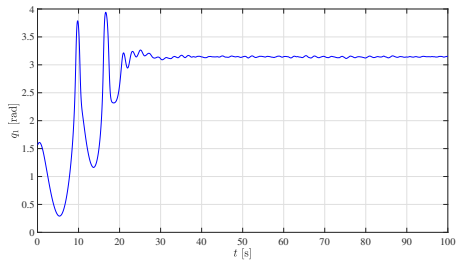

(a) Time history of q_1

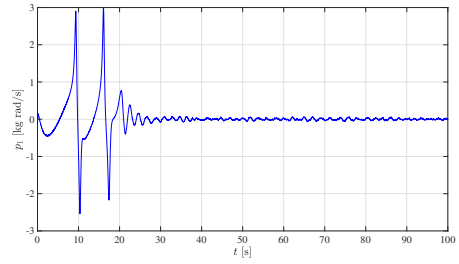

(b) Time history of p_1

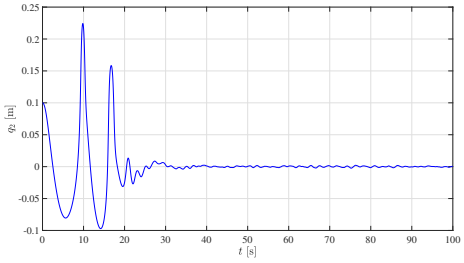

(c) Time history of q_2

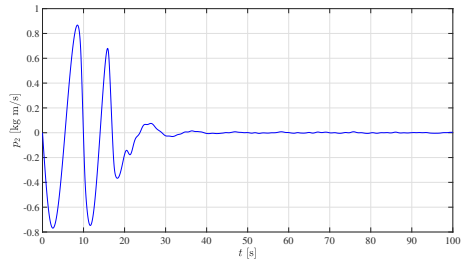

(d) Time history of p_2

Fig. 4. Case Study A. Time histories of the generalised coordinates and momenta during a test carried out in presence of parametric uncertainties, noisy measurements, and controller discretization.

5. CASE STUDY B: THE UNDERACTUATED COMPASS-LIKE BIPED ROBOT

5.1. Dynamic Model of the Underactuated Compass-Like Biped Robot

The compass-like biped robot (CBR) is a 2-DoF and bipedal walking robot belonging to the class of passive walkers (*i.e.*, robots capable of walking down a shallow slope without actuation, forced only by gravity). The stable walking exhibited by this class of systems is referred to as *passive gait*. This is due to the constancy of the mechanical energy during the whole gait, given by the restoration of mechanical energy which takes place at each impact between the robot legs and the ground, in hypotheses of perfectly inelastic interactions, as shown in [29] in his pioneering study. Differently from applications which are mainly based on the notion of *zero moment point* [30], the interest behind such a kind of passive robot is due to both the intrinsic energetic efficiency and the similarity to hu-

man walking [31], [32]. In particular, the CBR consists of two legs joined by the hip of mass $m_H > 0$. Each leg has mass $m > 0$ and length $l = a + b$, where $a > 0$ is the length of the legs between m and the feet while $b > 0$ is the length of the legs between m_H and m, supposing both m_H and m to be point masses. A full actuation version of the CBR can be considered to alter the passive gait. A representation of such a biped robot is depicted in Fig. 5.

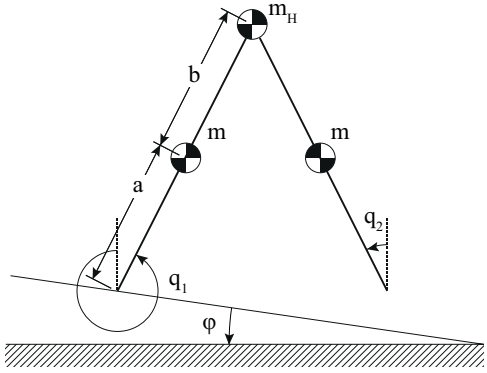

Fig. 5. Scheme of a compass-like biped robot.

Although its simple kinematic structure (*i.e.*, a double inverted pendulum with lumped masses on both legs and hip), the CBR exhibits a rich nonlinear dynamic due to the hybrid nature of the walking [33]. Due to the core role assumed by the restoration of mechanical energy in the generation of passive gait, it seems natural to employ passivity-based approaches to control such a kind of robot. One example, which starts from the Lagrangian model of the robot, is the work carried out in [34], where a potential energy shaping control based on the controlled-Lagrangian framework makes the biped's gait invariant to ground slope changes. A total energy shaping control, adequate to regulate the biped's forward speed as well as to increase the robustness of the walking in the presence of uncertainties on the initial conditions, is proposed in [35]. An underactuated version of the compass-like biped robot (UCBR) is introduced in [36] to demonstrate the effects of a kinetic energy shaping approach in terms of non-passive gait generation, realising rapid and long steps, and exhibiting proper robustness respect to uncertainties on the initial conditions. On the other hand, starting from the pH modelling framework, a methodology based on the IDA-PBC, which generates gaits characterised by slow and short steps, is applied in [31].

In this section, a UCBR model is served as a test-bed to demonstrate the effectiveness of the methodology presented in Section 3 to generate additional gaits to the passive one. No double-support phase is admitted (*i.e.*, only one leg at a time is in contact with the ground). The leg in contact with the ground is referred to as *support leg*, while the other one is referred to as *nonsupport leg*. Let q_1 be the actuated variable, that is the angle between the vertical relative to the ground and the support leg. Let q_2 be the unactuated variable, that is the angle between the vertical relative to the ground and the nonsupport leg. The relative momenta are denoted by p_1 and p_2, respectively. The behaviour of the UCBR consists of two distinct phases. The former phase, called *swing phase*, represents the behaviour of the UCBR before that the nonsupport leg hits the ground. It is described by (1) with the elements of the inertia matrix $M(q)$ as

$$\begin{aligned} &b_{11} = (m_H + m)l^2 + ma^2, b_{12}(q) = -mlb\cos(q_1 - q_2) \\ &b_{22} = mb^2, \end{aligned} \tag{43}$$

with $H(q)$ as in (2), where $V(q) = (m(a+l) + m_H l)g\cos(q_1) - mbg\cos(q_2)$ with $g \simeq 9.81$ m/s^2 the gravity acceleration. The latter phase, called *impact phase*, represents the instantaneous change in the angular velocities caused by the impact between the nonsupport leg and the ground. The impact occurs when the conditions

$$\begin{aligned} &y_h(q) = l[\cos(q_1 + \varphi) - cos(q_2 + \varphi)] = 0, \\ &\dot{y}_h(q) = l[\sin(q_2 + \varphi)\dot{q}_2 - sin(q_1 + \varphi)\dot{q}_1] < 0, \end{aligned} \tag{44}$$

hold, with $y_h \in \mathbb{R}$ the distance between the nonsupporting foot and the ground. Such a change, assuming perfectly inelastic and non-slipping contact between the nonsupporting foot and the ground, as well as an instantaneous transfer from supporting to nonsupporting one (no double-support phase admitted), is described by $\dot{q}(t^+) = P(q(t^-))\dot{q}(t^-)$, where $\dot{q} = \begin{bmatrix}\dot{q}_1 & \dot{q}_2\end{bmatrix}^T \in \mathbb{R}^2$ is the velocity vector, while the time instants just before and just after the impact are given by t^- and t^+, respectively. The conservation of angular momentum law is used to derive the expression of the matrix $P(q(t^-)) \in \mathbb{R}^{2\times 2}$, which is

$$P(q(t^-)) = \begin{bmatrix} p_{11}^+ & p_{12}^+ \\ p_{21}^+ & p_{22}^+ \end{bmatrix}^{-1} \begin{bmatrix} p_{11}^- & p_{12}^- \\ p_{21}^- & p_{22}^- \end{bmatrix}, \tag{45}$$

with $p_{11}^+ = ml(l - b\cos(q_1^- - q_2^-)) + ma^2 + m_H l^2$, $p_{12}^+ = mb(b - l\cos(q_1^- - q_2^-))$, $p_{21}^+ = -mbl(\cos(q_1^- - q_2^-))$, $p_{22}^+ = mb^2$, $p_{11}^- = -mab + (m_H l^2 + 2mal)\cos(q_1^- - q_2^-)$, $p_{12}^- = p_{21}^- = -mab$, $p_{22}^- = 0$. Since the UCBR exhibits a gait with left-right symmetry, at each impact the angles are swapped and relabelled (*i.e.*,when an impact occurs, the former nonsupport leg becomes the support one and vice-versa). Hence, these angles are not associated with a physical leg, but they are referred to as the action played by the leg during the gait. This procedure is taken into account via the matrix $R = \begin{bmatrix} 0 & 1 \\ 1 & 0 \end{bmatrix}$ which results in $q^+ = Rq^-$ at each impact. In the literature regarding biped locomotion, two parameters are introduced to describe the gait synthetically: namely, the step length S and the

period T. The former is the step length evaluated every two consecutive impacts between the nonsupport foot and the ground, and the latter is the time interval occurring between two consecutive impacts (*i.e.*, the duration of each every single step). The interested reader can refer to the work in [33] for further details. Hence, the UCBR hybrid behaviour is given by the composition of the swing and the impact phases.

5.2. Control Design for the UCBR

The following procedure assumes $k_1 = 0$ and $k_2 \neq 0$. The introduction of a controller, which exerts his action during the swing phase, gives birth to gaits that the uncontrolled UCBR cannot exhibit unless to change the mass/geometrical properties of the robot and/or the slope of the surface on which the robot walks. These artificial gaits are associated to several limit cycles in the state space of the UCBR. These limit cycles, representing the asymptotic behaviour of the closed loop, are due to the impacts between the nonsupport leg and the ground. The analytical detection of such periodic solutions is a difficult task, as the stabilisation of the asymptotic motion of the robot to the desired limit cycle, namely the *orbital stabilization* problem [37]. The goal of this section is neither the stabilisation of the system to the desired equilibrium point, nor the orbital stabilisation to the desired limit-cycle. Conversely, this section aims to show that the introduction of a total energy shaping control action, like the one presented in this work, effectively generates gaits which cannot be exhibited by the uncontrolled biped and whose stability is verified numerically a posteriori.

To get a proper function $\gamma(q_1)$, a constant $f_3(q_1) = -1/k_2^2$ function is picked up. With such a choice, results that $\gamma(q_1) = -1/k_2^2$. Then, choosing the function $f_1(q_1)$ in (30) as $f_1(q_1) = k_3(ma + (m+m_h)l)g\cos(q_1)$, with $k_3 \in \mathbb{R}$ a suitable gain, the desired potential energy in (30) becomes $V_d(q) = -k_2 bmg\cos(q_2) + k_3 g(ma + (m+m_H)l)\cos(q_1)$. Notice that the two gains k_2 and k_3 weigh the components of the original system's potential energy relative to the nonsupporting and the supporting leg, respectively. Since the UCBR without the impact resembles a double inverted pendulum, the most natural choice seems to assign $q^* = \begin{bmatrix}\pi & 0\end{bmatrix}^T$ as equilibrium, like the one in the mathematical model of the plant. In fact, the sought goal is not to stabilise the system at the desired equilibrium but rather to generate new gaits. The gradient of $V_d(q,c_2)$ is

$$\nabla_q V_d(q,c_2) = \begin{bmatrix} -k_3(ma+(m+m_H)l)g\sin(q_1) \\ k_2 bmg\sin(q_2), \end{bmatrix} \quad (46)$$

which, evaluated in $q^\star$, becomes $\nabla_q V_d(q,c_2)\Big|_{q^\star} = 0_2$. The Hessian of $V_d(q,c_2)$, evaluated in $q^\star$, is

$$\nabla_q^2 V_d(q,c_2)\Big|_{q^\star} = \begin{bmatrix} k_3(ma+(m+m_H)l)g & 0 \\ 0 & k_2 bmg \end{bmatrix}. \quad (47)$$

This Hessian matrix is positive definite if the conditions $k_2 > 0$, $k_3 > 0$ hold. Therefore, if k_2 and k_3 are simultaneously positive, **C.2** is satisfied. The scalar functions $a_{12}(q)$ and $a_{22}(q)$ are evaluated using, respectively, (31a) and (31b) while the free term $a_{11}(q)$ is chosen as $a_{11}(q) = k_4 b_{11}/(k_2\Delta(q))$, with $k_4 \in \mathbb{R}$ a suitable gain. Thereby, the desired inertia matrix becomes

$$M_d(q,c_1) = \frac{1}{k_2}\begin{bmatrix} k_4 b_{11} & b_{12}(q) \\ b_{12}(q) & b_{22} \end{bmatrix}, \quad (48)$$

whose determinant is $\Delta_d(q) = (k_4 b_{11}(q) b_{22}(q) - b_{12}^2(q))/k_2^2$. To comply with **C.1**, it should be proven that the desired inertia matrix is positive definite. Thanks again to the Sylvester's criterion, this is true if both $a_{11}(q) > 0$ and $\Delta_d(q) > 0$. The former is true if both $k_2 > 0$ and $k_4 > 0$. On the other hand, the latter condition is true if $k_4 > (mlb)^2/(b_{11}b_{22})$. Hence, the choice

$$k_2 > 0, k_3 > 0, k_4 > \frac{(mlb)^2}{b_{11}b_{22}} \quad (49)$$

satisfies both **C.1** and **C.2**.

The scalar interconnection term $j_2(q,p)$, computed as in (22), has the following expression

$$j_2(q,p) = \frac{\psi_1(q,p) + \psi_2(q,p)}{\psi_3(q)}, \quad (50)$$

with

$$\begin{aligned}
\psi_1(q,p) &= b\, b_{11}(-1+k_4)lm(-8b_{11}^2 b_{22}^2 k_4 p_2 \\
&\quad + 3b^4 l^4 m^4 p_2 + 4b\, b_{22} lm(-2b_{11}b_{22}(1+k_4) \\
&\quad + 3b^2 l^2 m^2) p_1 \cos(q_1 - q_2)), \\
\psi_2(q,p) &= b\, b_{11}(-1+k_4)lm(4b^4 l^4 m^4 p_2 \cos(2(q_1 \\
&\quad - q_2)) + 4b^3 b_{22} l^3 m^3 p_1 \cos(3(q_1 - q_2)) \\
&\quad + b^4 l^4 m^4 p_2 \cos(4(q_1 - q_2))\sin(q_1 - q_2)). \\
\psi_3(q) &= 8k_2(b_{11}b_{22} - b^2 l^2 m^2 \cos(q_1 - q_2)^2)^2(b_{11}b_{22}k_4 \\
&\quad - b^2 l^2 m^2 \cos(q_1 - q_2)^2).
\end{aligned}$$

Both the denominator of (50) and the passive output are independent from the generalised momenta. The gains chosen as in (49) avoid any singularity depending on q, assuring that the denominator of (50) never becomes zero.

Notice that the terms b_{11}, b_{22}, and $b_{12}(q)$ were often not explicitly expressed due to space constraints. The total control action is given by (10).

5.3. Simulations for the Controlled UCBR

The current section aims to demonstrate the effectiveness of the designed controller for the UCBR in generating new gaits. The nominal dynamic parameters chosen

for the UCBR are $m_H = 10$ kg, $m = 5$ kg, $a = 0.5$ m, $b = 0.5$ m, $g = 9.8$ m/s^2, and $\varphi = 3$ deg. The objective is the generation of two different gaits which cannot be exhibited by the uncontrolled UCBR. Recalling the S and T parameters describing a generic gait, the formerly desired gait is characterised by a smaller step length S and a bigger period T: it will be referred to as *small gait*. The latter desired gait features an increased step length S and a reduced period T: it will be referred to as *large gait*. Tests are performed on a standard personal computer, using the Matlab *ODE*45 routine together with the event detection option active, to evaluate the hits between the nonsupporting foot and the ground. The controller is implemented at a discrete-time step of 0.01 s.

5.3.1 Case Study B-1: Small Gait

In order to generate the small gait, the controller is designed through the following set of gains $k_2 = 1.25$, $k_3 = 0.45$, $k_4 = 1.05$ and $k_d = 0.1$, experimentally tuned complying with (49). The simulation starts with initial conditions $q_0 = \begin{bmatrix} 0.2187 & -0.3234 & -1.0918 & -0.3772 \end{bmatrix}^T$ and is carried out for 30 s. As shown in Fig.6, the step length S and the step period T asymptotically converge to values 0.4871 m and 0.7854 s, which are respectively smaller and bigger than the parameters $S = 0.5347$ m and $T = 0.7347$ s characterising the passive gait. This last is generated by turning off the controller and using the same initial conditions.

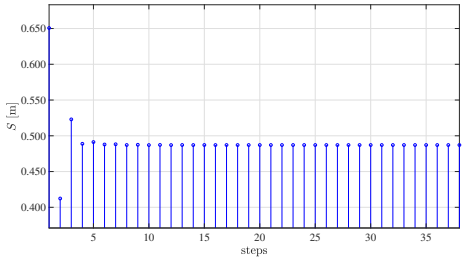

(a) Time history of S.

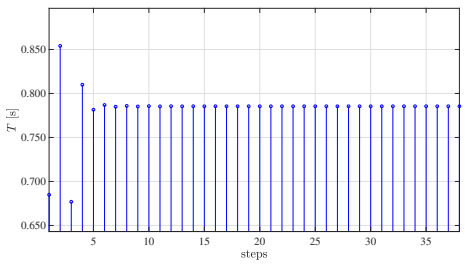

(b) Time history of T.

Fig. 6. Case Study B-1. Time histories of the step length and the step period with a controller generating a small gait.

5.3.2 Case Study B-2. Large Gait

Large gait is achieved by designing the controller with gains $k_2 = 0.8$, $k_3 = 1.1$, $k_4 = 0.9$ and $k_d = 0.0$, which fulfil again (49). The simulation, as for the small gait case study, starts with initial conditions $q_0 = \begin{bmatrix} 0.2187 & -0.3234 & -1.0918 & -0.3772 \end{bmatrix}^T$ and lasts for 30 s. Figure 7 depicts the step length S and the step period T which asymptotically converge to values 0.5387 m and 0.7322 m, which are respectively bigger and smaller than the parameters S and T characterising the passive gait.

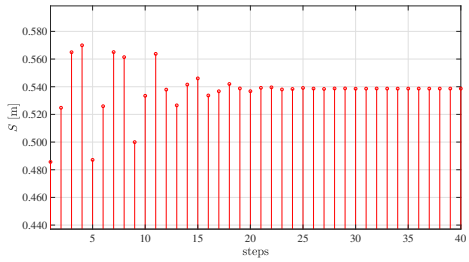

(a) Time history of S.

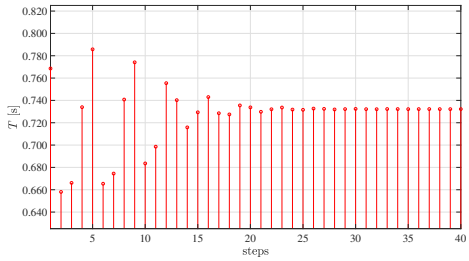

(b) Time history of T.

Fig. 7. Case Study B-2. Time histories of the step length and the step period with a controller generating a large gait.

5.3.3 Comparison Between the Small Gait and the Large Gait

Figure 8 represents the comparison between the limit cycles associated respectively to the small gait (the red one), the passive gait (the green one), and the large gait (the blue one). As a consequence of the designs proposed in the previous subsections, the small gait limit cycle is enclosed by the passive limit cycle, which is, in turn, contained by the large gait limit cycle.

6. CONCLUSION

In this paper, a constructive solution to deal with IDA-PBC for underactuated two-degree-of-freedom mechanical systems was introduced. The proposed strategy combines the attributes of the parameterised IDA-PBC with those of the algebraic IDA-PBC: *i)* it provides explicit solutions of the PDEs arising from the matching process

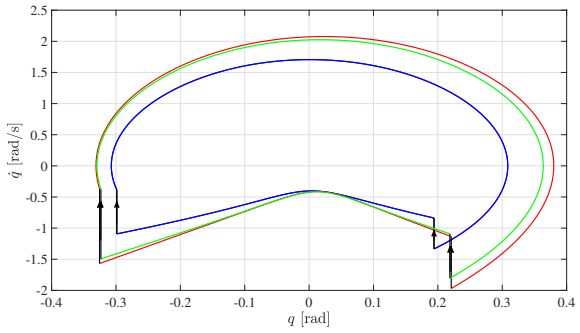

Fig. 8. Case Study B. Comparison between the passive-gait limit cycle (the green one), the small-gait limit cycle (the blue one), and the large-gait limit cycle (the red one). The black vertical lines indicate the resetting events at the impact between the nonsupporting leg and the ground.

without requiring the a priori knowledge of the desired total energy; *ii)* the singularity in the generalised momenta, usually appearing in the desired interconnection matrix within state-of-the-art methodologies is avoided; *iii)* it does not put any constraint on the structure of the original system's inertia matrix. For these reasons, the proposed methodology overcomes the limitations inherent to both parameterised IDA-PBC and algebraic IDA-PBC. It is indeed a useful tool in the control of two-degree-of-freedom mechanical systems with underactuation degree one. Numerical simulations are carried out on two well-known systems, namely, the TORA and the UCBR. The results remarked the high performance of such a new control strategy, as for the classical equilibrium point stabilisation as for the stable periodic gait generation. Future extensions of this paper aim to generalise the approach to systems with higher dimensions and higher underactuation degree.

FUNDING

The research leading to these results has been supported by both the PRINBOT project (in the frame of the PRIN 2017 research program, grant number 20172HHNK5_002) and the WELDON project (in the frame of Programme STAR, financially supported by UniNA and Compagnia di San Paolo). The authors are solely responsible for its content.

ACKNOWLEDGMENTS

The authors would like to thank Alejandro Donaire and José Guadalupe Romero for their support and the useful comments during the derivation of the work.

REFERENCES

[1] R. Ortega, A. Van Der Schaft, B. Maschke, and G. Escobar, "Interconnection and damping assignment passivity-based control of port-controlled Hamiltonian systems," *Automatica*, vol. 38, no. 4, pp. 585–596, 2002.

[2] S. Ganjefar, M. Afshar, M. H. Sarajchi, and Z. Shao, "Controller Design Based On Wavelet Neural Adaptive Proportional Plus Conventional Integral-Derivative For Bilateral Teleoperation Systems With Time-Varying Parameters," *International Journal of Control, Automation and Systems*, vol. 16, pp. 2405–2420, 2018.

[3] S. Ganjefar, M. H. Sarajchi, and M.-T. Hamidi Beheshti, "Adaptive sliding mode controller design for nonlinear teleoperation systems using singular perturbation method," *Nonlinear Dynamics*, vol. 81, pp. 1435–1452, 2015.

[4] M.-H. Sarajchi, S. Ganjefar, S. M. Hoseini, and Z. Shao, "Adaptive Controller Design Based On Predicted Time-delay for Teleoperation Systems Using Lambert W function," *International Journal of Control, Automation and Systems*, vol. 17, pp. 1445–1453, 2019.

[5] J. Qiu, J. Wenqiang, and M. Chadli, "A Novel Fuzzy Output Feedback Dynamic Sliding Mode Controller Design for Two-Dimensional Nonlinear Systems," *IEEE Transactions on Fuzzy Systems*, pp. 1–1, 2020.

[6] R. Ortega and E. Garcia-Canseco, "Interconnection and damping assignment passivity-based control: A survey," *European Journal of Control*, vol. 10, pp. 432–450, 2004.

[7] M. Zhang, R. Ortega, Z. Liu, and H. Su, "A new family of interconnection and damping assignment passivity-based controllers," *International Journal of Robust and Nonlinear Control*, vol. 27, no. 1, pp. 50–65, 2017.

[8] K. Nunna, M. Sassano, and A. Astolfi, "Constructive interconnection and damping assignment for port-controlled hamiltonian systems," *IEEE Transactions on Automatic Control*, vol. 60, no. 9, pp. 2350–2361, 2015.

[9] K. Fujimoto and S. Toshiharu, "Canonical transformations and stabilization of generalized Hamiltonian systems," *System & Control Letters*, vol. 42, pp. 217–227, 2001.

[10] R. Ortega, M. Spong, F. Gómez-Estern, and G. Blankenstein, "Stabilization of a class of underactuated mechanical systems via interconnection and damping assignment," *IEEE Transactions on Automatic Control*, vol. 47, no. 8, pp. 1218–1233, 2002.

[11] J.-A. Acosta, R. Ortega, and A. Astolfi, "Interconnection and damping assignment passivity-based control of mechanical systems with underactuation degree one," *IEEE Transactions on Automatic Control*, vol. 50, pp. 1936–1955, 2005.

[12] A. Donaire, R. Mehra, R. Ortega, S. Sumeet, J.-G. Romero, K. Faruk, and N.-M. Singh, "Shaping the energy of mechanical systems without solving partial differential equations," *IEEE Transactions on Automatic Control*, vol. 61, no. 4, pp. 1051–1056, 2016.

[13] D. Serra, F. Ruggiero, A. Donaire, L.-R. Buonocore, V. Lippiello, and B. Siciliano, "Control of nonprehensile planar rolling manipulation: A passivity-based approach," *IEEE Transactions on Robotics*, vol. 35, no. 2, pp. 317–329, 2019.

[14] P. Arpenti, F. Ruggiero, and V. Lippiello, "Interconnection and damping assignment passivity-based control for gait generation in underactuated compass-like robots," IEEE International Conference on Robotics and Automation, (Paris, F), 2020.

[15] P. Arpenti, D. Serra, F. Ruggiero, and V. Lippiello, "Control of the TORA system through the IDA-PBC without explicit solution of matching equations," 2019 Third IEEE International Conference on Robotic Computing (IRC), (Naples, Italy), 2019.

[16] Y. Liu and H. Yu, "A survey of underactuated mechanical systems," *IET Control Theory Applications*, vol. 7, no. 7, pp. 921–935, 2013.

[17] A. Van Der Schaft, "l_2-gain and passivity techniques in nonlinear control," Communications and Control Engineering, Berlin: Springer, 2017. ISBN 978-3-319-49991-8.

[18] M. Ryalat and D. Laila, "A simplified IDA—PBC design for underactuated mechanical systems with applications," *European Journal of Control*, vol. 27, pp. 1–16, 2016.

[19] F. Gómez-Estern and A.-J. Van der Schaft, "Physical Damping in IDA-PBC Controlled Underactuated Mechanical Systems," *European Journal of Control*, vol. 10, no. 5, pp. 451–468, 2004.

[20] C.-J. Wan, D.-S. Bernstein, and V.-T. Coppola, "Global stabilization of the oscillating eccenteric rotor," *Nonlinear Dynamics*, vol. 10, pp. 49–62, 1996.

[21] A. Morillo, M. R. Bolivar, and V. Acosta, "feedback stabilization of the TORA system via interconnection and damping assignment control," 17th IFAC World Congress, (Seoul, KR), pp. 3781–3786, 2008.

[22] D.-A. Dirksz, J. Scherpen, and R. Ortega, "Interconnection and damping assignment passivity-based control for port-Hamiltonian mechanical systems with only position measurements," 47th IEEE Conference on Decision and Control, (Cancun, MX), pp. 4957–4962, 2008.

[23] M. Jankovic, D. Fontaine, and P.-V. Kokotovic, "TORA example: Cascade and passivity-based control designs," *IEEE Transactions on Control Systems Technology*, vol. 4, no. 3, pp. 292–297, 1996.

[24] R. Olfati-Saber, "Nonlinear control and reduction of underactuted systems with symmetry I: Actuated shape variables case," 40th IEEE Conference on Decision and Control, (Orlando, FL, US), pp. 4158–4163, 2001.

[25] N. Qaiser, N. Iqbal, A. Hussain, and N. Qaiser, "Exponential stabilization of a class of underactuated mechanical systems using dynamic surface control," *International Journal of Control, Automation and Systems*, vol. 5, pp. 547–558, 2007.

[26] A. Pavlov, B. Jansen, N. van der Wouw, and H. Nijmeijer, "Experimental output regulation for the TORA system," 44th IEEE Conference on Decision and Control, (Sevilla, ES), pp. 1108–1113, 2005.

[27] T. Tanighuchi and M. Sugeno, "Piecewise multi-linear model based control for TORA system via feedback linearization," International MultiConference of Engineers and Computer Scientist, (Honk Kong, CN), 2018.

[28] K. Tanaka, T. Tanighuchi, and H.-O.-M. Wang, "Model-based fuzzy control of the TORA: Fuzzy regulator and fuzzy observer design via LMIs that rapresent decay rate, disturbance rejection, robustness, optimality," 1998 IEEE International Conference on Fuzzy Systems Proceedings., (Anchorage, AK, US), 1998.

[29] T. McGeer, "Passive dynamic walking," *International Journal of Robotic Research*, vol. 9, no. 2, pp. 62–82, 1990.

[30] E.-Z. Dong, D.-D. Wang, J.-G. Tong, C. Chen, and Z.-H. Wang, "A Stable Gait Planning Method of Biped Robot Based on Ankle motion Smooth Fitting," *International Journal of Control, Automation and Systems*, vol. 16, pp. 284–294, 2018.

[31] V. De-León-Gómez, V. Santibanéz, and J. Sandoval, "Interconnection and damping assignment passivity-based control for a compass-like biped robot," *International Journal of Advanced Robotic Systems*, vol. 14, no. 4, 2017.

[32] A.-D. Kuo, "The six determinants of gait and the inverted pendulum analogy: A dynamic walking perspective," *Human Movement Science*, vol. 26, no. 4, pp. 617–656, 2007.

[33] A. Goswami, B. Thuilot, and B. Espiau, "Compass-like biped robot Part I: Stability and bifurcations of passive gaits," *Institut National de Recherche en Informatiqu et en Automatique (INRIA),Techical Report 2996*, 1996.

[34] M.-W. Spong and F. Bullo, "Controlled symmetries and passive walking," Proceeding IFAC Triennal World Congress, (Barcelona, Spain), 2002.

[35] M.-W. Spong, J. Holm, and D. Lee, "Passivity-based control of bipedal locomotion," *IEEE Robotics & Automation Magazine*, vol. 12, no. 2, pp. 30–40, 2007.

[36] J. Holm and M.-W. Spong, "Kinetic energy shaping for gait regulation of underactuated bipeds," IEEE International Conference on Control Applications, (San Antonio, Texas, USA), pp. 1232–1238, 2008.

[37] A.-S. Shiriaev, L.-B. Freidovich, and S.-V. Gusev, "Transverse linearization for controlled mechanical systems with several passive degrees of freedom," *IEEE Transactions on Automatic Control*, vol. 55, no. 4, pp. 893–906, 2010.

[38] F. Ghorbel, B. Srinivasan, and M.-W. Spong, "On the uniform boundedness of the inertia matrix of serial robot manipulators," *Journal of Robotic Systems*, vol. 15, pp. 17–28, 1998.

APPENDIX A

1. EXISTENCE OF THE INTEGRALS

A.1. Existence of the integral within equation (20)

To guarantee a closed-form solution for the integral in (20), from the fundamental theorem of calculus, it is

necessary to show that the integrand is an integrable function. Since the continuity implies the integrability, in the Riemann sense, to accomplish the task, it is sufficient to show that the argument of the integral is a continuous function over the set $\begin{bmatrix}1 & q_1\end{bmatrix}$. The integrand of (20) is a fractional function. Notice that the quotient of two continuous functions is continuous if the denominator is not equal to zero. The numerator is the gradient of the plant's potential energy. Therefore, it is a conservative force that is continuous everywhere by definition ($V(q)$ is a class $\mathcal{C}_2$ function due to its relationship with the Hamiltonian). Regarding the continuity of the denominator, specific conditions will be expressed in the next subsection. As a matter of fact, the integrand's continuity in (20) is strongly related to the integrand's continuity in (26).

A.2. Existence of the integral within equation (26)

Starting from the considerations provided in the previous subsection, the integrand of (26) is a fractional function too. The numerator and the denominator are continuous because they are a linear combination of the plant's inertia matrix terms and their gradients. Hence, the continuity of the integrand reduces to avoid that the denominator becomes zero, as given by the following condition

$$k_1 b_{12}\left(\begin{bmatrix}\sigma & f_4(q,\sigma)\end{bmatrix}\right)+k_2 b_{22}\left(\begin{bmatrix}\sigma & f_4(q,\sigma)\end{bmatrix}\right)\neq 0,$$

which yields to

$$k_2 \neq -\frac{k_1 b_{12}\left(\begin{bmatrix}\sigma & f_4(q,\sigma)\end{bmatrix}\right)}{b_{22}\left(\begin{bmatrix}\sigma & f_4(q,\sigma)\end{bmatrix}\right)}. \tag{A.1}$$

It is thus necessary to find upper and lower bounds for k_2 to satisfy (A.1). This is equivalent to compute the bounds for $b_{12}(q_1,q_2)$ and $b_{22}(q_1,q_2)$. Such bounds exist if and only if $M(q)$ is bounded too. A study about the boundedness of the inertia matrix of serial robot manipulators was carried out in [38]. At the same time, several examples are provided for many underactuated 2-DoF mechanical systems (the Acrobot, the Pendubot, the cart-pole, the crane, the rotating pendulum, the inertia-wheel pendulum, the magnetic suspension, the ball-and-beam, and the TORA) [16], that are precisely the target of this paper (where the compass-like biped robot is added to the list, and others can be found in the literature). Moving from this assumption, it is possible to always satisfy (A.1) through the following (very) conservative condition

$$k_2 > \left|\frac{k_1 \max\left(b_{12}\left(\begin{bmatrix}\sigma & f_4(q,\sigma)\end{bmatrix}\right)\right)}{\min\left(b_{22}\left(\begin{bmatrix}\sigma & f_4(q,\sigma)\end{bmatrix}\right)\right)}\right|, \tag{A.2}$$

where the given bounds exist due to the boundedness of $M(q)$. Hence, the integral in (26) exists and it is well-defined. In turn, this yields to the existence of the integral in (20). As a matter of fact, $f_2(q,c_1)$ in (26) cannot be zero since it is an exponential continuous function. Therefore, the function $\gamma(q,c_1)$ in (25) cannot be zero since $f_3(\cdot,\cdot)$ is a nonzero continuous function. Since the product of a finite number of continuous functions is still a continuous function, and since $\gamma(q,c_1)$ cannot be zero, the denominator in (20) is a nonzero continuous function. This yields to the existence of the integral in (20).

Pierluigi Arpenti received the M.Sc. degree in Automation Engineering from the University of Naples Federico II in 2016. Currently, he is a Ph.D. candidate in Information Technologies and Electrical Engineering at the same university. His research interests are focused on passivity-based control, underactuated mechanical systems, legged robots, and robotics for logistics and manufacturing.

Fabio Ruggiero received the M.Sc. degree in Automation Engineering from the University of Naples Federico II in 2007. He got the Ph.D. degree from the same institution in 2010. He spent seven months at Northwestern University as a visiting Ph.D. student from September 2009 to March 2010. After several PostDoctoral positions from 2011 to 2016, he has been holding an Assistant Professor position at the University of Naples Federico II. His research interests are focused on dexterous and dual-hand robotic manipulation, even by using UAVs with small robotic arms, dynamic nonprehensile manipulation, legged robotics. He has co-authored more than 50 among journal papers, book chapters, and conference papers.

Vincenzo Lippiello was born in Naples, Italy, on June 19, 1975. He received his Laurea degree in electronic engineering and the Research Doctorate degree in information engineering from the University of Naples Federico II, in 2000 and 2004, respectively. He is Professor of Automatic Control in the Department of Electrical Engineering and Information Technology, University of Naples Federico II. His research interests include visual servoing of robot manipulators, hybrid visual/force control, adaptive control, grasping and manipulation, aerial robotics, and visual object tracking and reconstruction. He has published more than 120 journal and conference papers and book chapters.